

Phytoconstituents of *Cassia auriculata* Linn Inhibits the Pro-Inflammatory Cytokines: An *In Silico* Study to Identify Multi-Target Drug Candidates

Tejaswini R H ¹, Shivaleela Biradar ¹, Shreedevi S J ¹, Dr. Devaraju K S ², Dr. Babu R L ^{1,*}

¹ Laboratory of Natural Compounds and Drug Discovery, Department of Bioinformatics, Karnataka State Akkamahadevi Women University, Vijayapura-586108, Karnataka, India; tejaswini.teju112@gmail.com (T.R.H.); shivaleelabiradar4@gmail.com (S.B.); sridevij539@gmail.com (S.S.J.);

² Department of Biochemistry, Pavate Nagar, Karnataka University, Dharwad, Karnataka, India; devarajuks@gmail.com(DKS);

* Correspondence: babu@kswu.ac.in (B.R.L.);

Scopus Author ID 9036899400

Received: 21.10.2023; Accepted: 7.07.2024; Published: 24.09.2024

Abstract: Inflammation is the most essential part of the body's immune system and is responsible for diseases manifestation in asthma, rheumatoid arthritis, allergy, aging, autoimmune diseases, etc. During these conditions, many cytokines were regulated. The pro-inflammatory cytokines play an essential role in the development of an effective defense against disease infections and progression. The early responsive cytokines such as IL-1beta, IL-6, and TNF-alpha are considered to identify effective inhibitors. The aim of this study is to screen the potential and precise phytoconstituents from ethnomedicinally important *Cassia auriculata* Linn, which may have potential inhibitors for pro-inflammatory targets. Methanol extract of *Cassia auriculata* Linn leaf was subjected to HR-LCMS analysis, the phytochemical signature was analyzed, and 85 phytochemicals were taken for the molecular docking studies with pro-inflammatory markers. After the screening, 11 compounds showed good binding energy with hydrogen bond interaction with three targets from the ADME property prediction 9 compounds showed parameter values within an acceptable range. Toxicity prediction reveals the 7 compounds are non-toxic. *In silico* investigations revealed that 7 phytoconstituents potentially inhibit the pro-inflammatory cytokines. In addition, two compounds are considered multi-targeted drugs inhibiting the three cytokines.

Keywords: *Cassia auriculata* Linn; pro-inflammatory cytokines; interleukin (IL); tumor necrosis factor-alpha (TNF-alpha); ethnomedicine; high resolution-liquid chromatography-mass spectrometry (HR-LCMS).

© 2024 by the authors. This article is an open-access article distributed under the terms and conditions of the Creative Commons Attribution (CC BY) license (<https://creativecommons.org/licenses/by/4.0/>).

1. Introduction

Ethnomedicine or traditional medicines are great contributors to the management of diseases in nearly 75-80% of the world population, and they have a long history of practice. Because of their safety, efficiency, and fewer side effects, herbal medications are becoming more and more popular in the 21st century [1]. Various herbal products have been used to treat and prevent diseases over the years, with varying degrees of effectiveness. Most of the world's population receives its primary healthcare from medicinal plants, which continue to be an essential therapeutic tool in the fight against most diseases. Ethnomedicine is mainly based on medicinal plants and their components, namely bioactive phytoconstituents. To create a range

of therapeutic agents, ancient people were compelled to investigate their local natural surroundings and significantly use several plant-based, animal-based, and mineral-based products in their quest for lifelong health and pain relief [2].

Cassia auriculata Linn belongs to the *Caesalpinaceae* (Fabaceae) family. In Indian ethnomedicine, this plant is commonly known as ‘Tanner’s Cassia’ or ‘Avartaki’ called in Ayurveda, ‘Avaram’, ‘Avarike’, ‘Taravada’, ‘Aval’ and ‘Hemapushpam’ [3]. It is found throughout wasteland in Asia. This plant species has been used in traditional Ayurvedic medicine to heal or relieve simple problems like gum and teeth pain, ulcers, fractures, soreness, and snakebite pain. The different parts of the *Cassia auriculata* Linn plant have been reported for its use in managing several therapeutic properties like anti-inflammation, antimicrobial, wound healing, local anesthetic smooth muscle relaxant activities, etc. [4-6]. Therefore, it is very important to know precise phytoconstituents to improve therapeutic usage, as using crude extract or crude material for the treatment may have side effects or reduced efficacy. To address the limitation, our study attempts to determine the active Phytoconstituents for anti-inflammatory properties [7].

Inflammation is a major driver and important process of the immune system responsible for the pathogenesis of a cluster of diseases that includes asthma, allergy, aging, rheumatoid arthritis, cancer, stroke, autoimmune diseases, as well as neurodegenerative and cardiovascular disease [8]. Inflammation was understood by a few key characteristics by the ancients: rubor (redness), dolor (pain), tumor (swelling), calor (heat), and functionless (loss of function) [9]. Instead of resistance and failure of the inflammatory response, which can result in damage and organ dysfunction, the typical outcome of an acute inflammatory process is the effective resolution and repair of tissue damage. Chronic dysplastic inflammation, autoimmunity, and excessive tissue damage can occur from acute inflammation that is not resolved, and this is something that may be expected [10]. During the process of inflammation, the expression of many cytokines is regulated. Endogenous chemical mediators called cytokines are crucial for controlling the body's inflammatory response. Pro-inflammatory cytokines originate predominantly from activated macrophages that are upregulated during inflammation. Cytokines such as Interleukin (IL)-1, IL-1, IL-6, IL-12, IL-17, IL-18, IL-23, tumor necrosis factor (TNF-alpha), BAFF, and interferon (IFN) are pro-inflammatory cytokines that are key factor initiating an efficient response against exogenous pathogens. Pro-inflammatory mediators are alienated by anti-inflammatory cytokines (IL-4, IL-10, IL-13, and TGF) [11,12], mainly IL-1 β , IL-6, and TNF-alpha are the early responsive pro-inflammatory cytokines which are commonly involved in various inflammatory diseases [13]. Therefore, as inflammatory cytokines are critical factors for the manifestation of inflammation, our study is focused on determining the precise phytoconstituents that can inhibit the selected pro-inflammatory cytokines. In the current study, the leaf extract of *Cassia auriculata* Linn is prepared using *methanol* and subjected to LCMS analysis. Then, identified compounds were subjected to various *in silico* tools to understand the inhibitory effects against early responsive cytokines (IL-1 β , IL-6, and TNF-alpha). A preliminary investigation of our study suggested 7 phytoconstituents potentially inhibit the pro-inflammatory cytokines. In addition, two phytoconstituents such as (Kaempferol and N-(3-Benzooxazol-2-yl-4-hydroxy-phenyl)-2-ptolyloxyacetamide) compounds are considered as multi- targeted drugs inhibiting all three cytokines.

2. Materials and Methods

2.1. Plant sample collection.

Cassia auriculata Linn plant is collected from the premises of Karnataka State Akkamahadevi Women University, Vijayapura (KSAWU), Karnataka, and authenticated by the Department of Botany, KSAWU, Karnataka, by referring to Madras flora. The fresh and healthy plant of *Cassia auriculata* Linn leaves are separated, then washed with running tap water, followed by distilled water, and dried properly in the shade for 1-2 weeks to remove the moisture. Further, leaves were crumbled by a mechanical grinder and passed through a 40 mm size mesh sieve [14]. The powdered leaves material was stored in an airtight container and used for further studies.

2.2. Preparation of extracts.

About 60 gm of shade-dried leaves powder of *Cassia auriculata* Linn was extracted in Soxhlet assembly with methanol solvent (polarity index: 5.1, boiling point: 64.7°C) not exceeding the boiling point. The 48 hours of extract was concentrated under reduced pressure in the rotary vacuum evaporator. The extract obtained with methanol solvent was weighed, and the percentage yield was calculated in terms of the dried weight of the leaf powder of the plant [15].

2.3. Identification of phytochemical profile by HR-LCMS.

The phytochemical profile of the obtained crude methanolic extract from *Cassia auriculata* Linn leaves was analyzed using high resolution-liquid chromatography-mass spectroscopy method (Instrument- HRLCMS-qToF-agilent Technologies, USA). The data acquisition software is Agilent Mass Hunter. Data Processing Software: Agilent Masshunter Qualitative Analysis B.06. Column details are ZORBAX Eclipse Plus -C18 150 x 2.1 MM, 5 microns (Agilent). The solvents used solvent A, 0.1% formic acid in Milli-Q water, and solvent B as acetonitrile. Ion mode is dual AJS ESI. MS-resolution power minimum range 200 m/z. The mass resolution threshold is 0.010 %. The column temperature is 40°C, and the injection volume is 5 µL. The 85 phytoconstituents resulted in HR-LCMS [16] (Performed at SAIF, IIT Mumbai, India).

2.4. Ligand preparation.

The 85 phytoconstituents of *Cassia auriculata* Linn were selected for virtual screening and molecular docking study against pro-inflammatory cytokines. The 3D structure of 85 phytoconstituents is retrieved from a database called PubChem (<https://pubchem.ncbi.nlm.nih.gov/>) [17]. Using the LigPrep of Schrödinger maestro, the ligands were prepared. Ligands were converted from 2D to 3D structures by including tautomeric variations, ionization, stereochemical, energy minimization, and optimization for ligands geometry, desalted and corrected for ligands chiralities and missing hydrogen atoms. Ligands bond orders were fixed and neutralized of charged groups. The tautomeric and ionization states were generated between 6.8 and 7.2 pH using the Epik module [18]. The Lipinski rule of 5 was checked based on analyzing four consistent physicochemical properties of ligands. These properties are molecular weight (MW) is ≤500 Dalton (Da), and the octanol/water partition coefficient (logP) is ≤ 10 [19].

2.5. Protein structure preparation.

The main pro-inflammatory cytokines IL-6 (PDB ID-1ALU) [20], IL-1beta (PDB ID-1ITB) [21], and TNF-alpha (PDB ID-7JRA) [22] were retrieved from the PDB database (Protein Data Bank) [23]. The proteins are prepared by a protein preparation wizard (standard method). In that, the bond order, formal charges, missing hydrogen atoms, topologies, and incomplete and terminal amide groups of protein structures are refined. Beyond the hetero atoms 5 Å, the water molecules were eliminated. For the heteroatom found in the protein structure, potential ionization states were produced, and the most stable state was selected. The hydrogen bonds were allocated, and the retained water molecules' orientations were adjusted. The protein structure was then cautiously minimized using the OPLS2005 force field to reposition side-chain hydroxyl groups and prevent potential steric conflicts. A predetermined Root Mean Square Deviation (RMSD) tolerance of 0.3 Å limits the minimization of the supplied protein coordinates [18].

2.6. Active site prediction.

The SiteMap module from the Schrodinger package was used to identify and characterize proteins' active sites and binding residues. In the first step of the SiteMap calculation, one or more sites on the protein surface that might be favorable for ligand binding to the receptor are found and described using grid position points. In order to aid in the molecular docking process with protein and ligand research, contour maps that produced hydrophilic and hydrophobic hydrogen bonding possibilities were created [24].

2.7. Molecular docking analysis.

After the preparation of ligands and receptors, the glide docking analysis was carried out using the previously prepared receptor grid and the ligand molecules in the Schrodinger maestro package. The approving interactions between ligand and receptor were scored by the GLIDE ligand docking module. For GLIDE [25], the three separate molecular docking modes were used sequentially: HTVS (high-throughput virtual screening) docking and scoring, SP (standard precision) docking and scoring, and XP (extra precision) docking and scoring. Using XP mode, all docking calculations concluded. A flexible docking method that automatically creates conformations for each ligand was used to progress the docking. The poses are produced by hierarchical filters that assess how ligands interact with proteins or receptors. Most comparable docking conformations contained the lowest-energy docked complexes [26].

2.8. ADME/T properties prediction.

The in-silico ADME properties of the proposed ligands were determined by using the QikProp module of Schrödinger software Maestro. The pharmacokinetics and pharmacodynamics of the ligands are studied using QikProp guidance to ascertain the drug-like properties. Predicted important ADME characteristics like Molecular weight: (acceptable range: ≤ 500), aqueous solubility: QPlogS ($-6.5 < x < 0.5$), apparent Caco-2 cell permeability in nm/sec: QPPCaco (nm per sec; 500 great), Conformation-independent predicted aqueous solubility, log S. S in mol dm⁻³:CIQPlogS ($-6.5 < x < 0.5$), metabolism: #metab (1–8), rule of three: ro3 (0), Central Nervous System permeability: CNS ($-2 =$ completely inactive, $-1 =$ very low activity, $0 =$ low activity, $1 =$ medium activity, $2 =$ completely active), QPlogKp: ($-8 < x < -5$), and brain/blood partition coefficient: QPlogBB ($-3.0- 1.2$) [19]. The toxicity of selected

compounds was predicted using the ProTox-II online server [27]. Different toxicity endpoints, including acute toxicity, hepatotoxicity, carcinogenicity, mutagenicity, and others, are predicted using the ProTox-II tool. SDF (structural data file) and SMILES (simplified molecular-input line-entry system) were used throughout the generation of the creation method. Computing the toxicity dosages has become relatively simple compared to estimates based on animal models because it can save the time required for experiments on animals [28].

2.9. Binding free energy calculation by using prime/MM-GBSA approach.

MM-GBSA (Molecular Mechanics-Generalized Born Surface Area) processes the binding free energies of the protein-ligand complex using the Schrödinger Suite 2018-4 Prime module. The complexes were refined with Prime under the OPLS 3e force field, adopting the Variable Dielectric Surface Generalized Born (VSGB) continuum solvation model [29]. The top compounds that were retrieved from the docking procedure then underwent the G scores. $\Delta G_{\text{binding}}$ was calculated for the protein-ligand complexes using MM-GBSA analysis available in the Prime module of GLIDE.

$\Delta G_{\text{binding}}$ was calculated based on the following formula:

$$\Delta G_{\text{binding}} = G_{\text{complex}} - (G_{\text{receptor}} + G_{\text{ligand}})$$

$$\Delta G_{\text{binding}} = \Delta E_{\text{MM}} + \Delta G_{\text{GB}} + \Delta G_{\text{SA}}$$

$\Delta G_{\text{binding}}$ = energy of the minimized complex – (energy of the minimized receptor + energy of the minimized ligand) [30].

3. Results and Discussion

3.1. Plant extraction.

About 60 gm of shade-dried leaf powder of *Cassia auriculata* Linn was extracted in Soxhlet assembly with 250 ml of methanol solvent. The extract obtained with methanol solvent was weighed. The yield of plant extract is found to be 8 grams.

3.2. Phytochemical profile by HR-LCMS.

The HR-LCMS studies of *Cassia auriculata* Linn leaf methanol extract revealed the presence of 85 compounds listed in Table 1. The structures of 85 compounds are retrieved from the PubChem database—the analysis of compounds performed in ESI positive and negative mode ionization [31]. Compounds are detected in ESI +ve, shown in Figure 1, and compounds detected in ESI -ve, shown in Figure 2.

Table 1. List of compounds detected in HR-LCMS.

Compounds are detected in ESI +ve ionization		Compounds are detected in ESI -ve ionization	
1	beta-D-Galactopyranosyl-(1->4)-beta-D-galactopyranosyl- (1->4)-D-galactose	1	2-Hydroxy-3-chloropenta-2,4-dienoate; 2,6-dihydroxybenzoic acid
2	Pirbuterol	2	Mecarbinzid
3	2,3-Butanediol glucoside	3	Crosatoside B
4	Miserotoxin	4	Gallic acid
5	Epigallocatechin	5	Glycophymoline
6	Methyl N-methylanthranilate	6	(+)-Galocatechin
7	Americanin B	7	Resorcinol
8	3alpha,4,7,7alpha-Tetrahydro4-hydroxy-1H-isoindole1,3(2H)-dione	8	Glyceryl lactopalmitate
9	Dulxanthone B	9	Saphenamycin
10	(5alpha,8beta,9beta)-5,9-Epoxy-3,6-megastigmadien-8-ol	10	N-(3-Benzooxazol-2-yl-4- hydroxy-phenyl)-2-ptolyoxyacetamide

Compounds are detected in ESI +ve ionization		Compounds are detected in ESI -ve ionization	
11	1,3,5,8-Tetrahydroxy-6- methoxy-2- methyl anthraquinone 8-O-b-Dglucoside	11	p-Hydroxyphenylbutazone
12	Rehmaionoside C	12	Sulfadoxine
13	Jasmolone glucoside	13	Vanillic acid
14	6-Hydroxykaempferol 6,7- diglucoside	14	Methotrimeprazine
15	Quercetin	15	Sulfadoxine
16	Isoorientin 7-glucoside	16	Pedaliin
17	Hyperoside	17	Gambiriin A3
18	Fabianine	18	Albanol A
19	Maritimetin	19	Protoaphin aglucone;
20	Ethyl 7-epi-12- hydroxy jasmonate glucoside	20	Myricitrin
21	Xanthoaphin	21	Cefoselis
22	4,7-Didehydroneophysalin B	22	Protoaphin aglucone
23	Polysorbate 20	23	Orcein
24	Belladonnine	24	7-Methyl-1,4,5-naphthalenetriol 4-[xylosyl-(1- >6)-glucoside]
25	Auriculine	25	Isonocardicin A
26	Retapamulin	26	Gladiatoside C2
27	19-Noretiocholanolone	27	5,7,8,3',4'- Pentahydroxyisoflavone
28	17-Hydroxylinolenic acid	28	Kaempferol
29	1,3-Diacetoxy-4,6,12- tetradecatriene-8,10-diyne	29	Atractyloside
30	D-Urobilin	30	Aurasperone D
31	Melongoside G	31	Hordatine A
32	Androsterone	32	Cytochalasin Npho
33	Flavidulol C	33	all-trans-heptaprenyl diphosphate
34	Avermectin B2a monosaccharide	34	Triamcinolone hexacetoneide
35	Erythromycin E	35	(2S,2'S)-Oscillool 2,2'-di(α-Lfucoside)
36	Phaeophorbide b		
37	Asparanin B		
38	9Z-Octadecen-12-ynoic acid		
39	23-Acetoxyisoladulcidine		
40	3-(5,6,6- Trimethylbicyclo[2.2.1]hept-1-yl)cyclohexanol		
41	Harderoporphyrin		
42	Campesteryl p-coumarate		
43	Harderoporphyrin		
44	Leukotriene F4		
45	DG(18:4(6Z,9Z,12Z,15Z)/18:4 (6Z,9Z,12Z,15Z)/0:0)		
46	Pheophorbide a		
47	16beta-Hydroxysteroid		
48	Allosamidine		
49	Euphornin		
50	3-cis-Hydroxy-b,e-Caroten-3'- one		

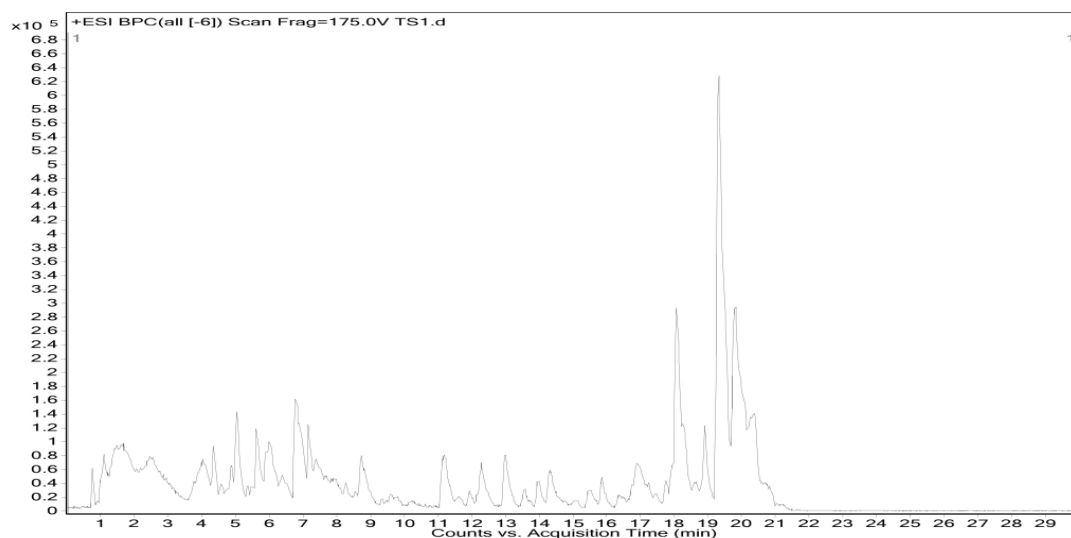


Figure 1. LC-MS chromatogram of methanolic Leaves extract of *Cassia auriculata* Linn on +ve ionization.

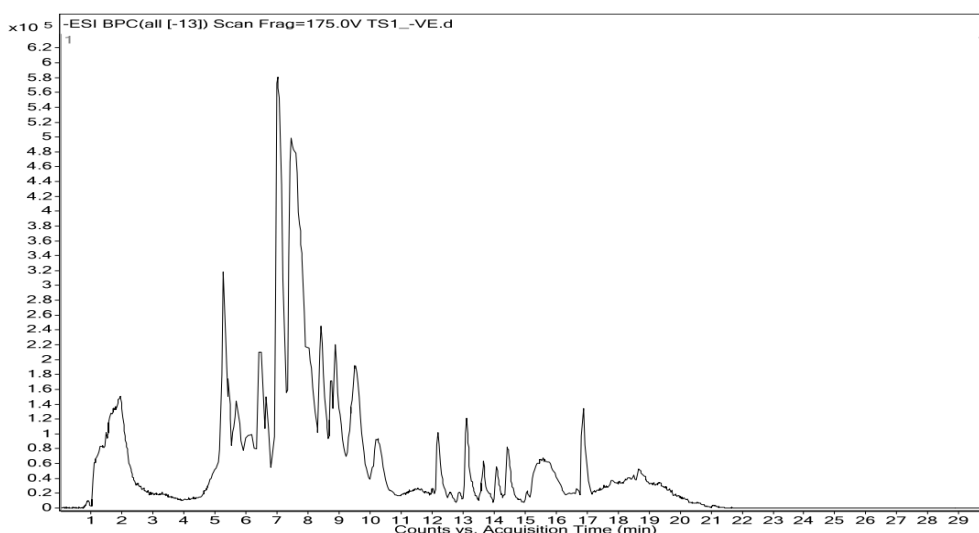


Figure 2. LC-MS chromatogram of methanolic Leaves extract of *Cassia auriculata* Linn on -ve ionization.

3.3. Ligand preparation.

The 85 phytochemicals were optimized using LigPrep. As a result, a total of 1022 conformations were obtained. The evaluation of drug-likeness was performed based on ‘Lipinski’s rule of five’ (ro5). 486 compounds obeyed Lipinski’s rule of five filtration. The filtered compounds are proceeded to perform protein-ligand docking [32].

3.4. Protein preparation.

An X-ray crystallography structure of IL-6 (PDB ID-1ALU), IL-1beta (PDB ID-1ITB), and TNF-alpha (PDB ID-7JRA) is obtained by the PDB database. Protein Preparation Wizard was used to prepare the protein structure for docking. The protein was prepared by removing water molecules, generating states using Epik, assigning bond order, allocate hydrogen bonds [33]. The energy minimization of structure using force field OPLS3. The Receptor Grid Generation is used for the structure binding site to set a grid box [18]. After protein preparation, the protein-ligand docking is performed.

3.5. Molecular docking.

Virtual screening can now positively impact the discovery process because of advances in computational techniques. The binding mechanisms of compounds to the amino acids found in the protein active pocket were examined using a grid-based docking analysis. To evaluate and identify the potential palliative lead molecule, subjected to glide docking analysis by Schrodinger suite, the active 85 phytochemicals of *Cassia auriculata* leaves with three main pro-inflammatory cytokines such as IL-6, IL-1beta, and TNF-alpha. The results of docking analysis are described in Table 2.

Table 2. Docking results of *Cassia auriculata* Linn phytochemicals with pro-inflammatory cytokines.

Si. No	Compound name(XP)	Targets	Docking score	Glide g-score	Glide e-model
1	Gallic acid	IL-6	-5.850	-5.850	-38.535
		IL-1beta	-7.611	-7.611	-43.798
2	Mecarbinzid	IL-6	-5.312	-6.190	-52.261
		IL-1beta	-8.560	-9.364	12.938
3	Maritimetin	IL-6	-5.199	-5.199	-29.358
		IL-1beta	-8.532	-8.532	-37.621
		TNF-alpha	-11.739	-11.739	-29.127
4		IL-6	-5.118	-5.118	-53.864

Si. No	Compound name(XP)	Targets	Docking score	Glide g-score	Glide e-model
	N-(3-Benzooxazol-2-yl-4-hydroxy-phenyl)-2-Ptoloyloxyacetamide	IL-1beta	-5.029	-5.338	-52.947
		TNF-alpha	-8.438	-8.747	-23.808
5	2,6-dihydroxybenzoic acid	IL-6	-4.956	-4.956	-51.318
		IL-1beta	-6.399	-6.399	-41.919
6	Methyl N- methyl anthranilate	IL-6	-4.404	-4.404	-18.390
		IL-1beta	-6.467	-6.467	-32.250
7	Kaempferol	IL-6	-4.270	-4.270	-30.047
		IL-1beta	-7.813	-7.813	8.229
		TNF-alpha	-11.425	-11.425	-30.639
8	Vanillic acid	IL-6	-3.834	-3.834	-14.293
		IL-1beta	-6.140	-6.140	-30.867
9	Resorcinol	IL-6	-3.011	-3.011	-35.838
10	2-Hydroxy-3-chloropenta-2,4- dienoate	IL-1beta	-6.140	-6.140	-30.867
11	Glycophymoline	TNF-alpha	-8.628	-8.643	-41.163

3.6. ADME prediction.

The 11 phytochemicals were finalized from docking results, which proceeded for ADME property prediction. The ADME properties are assessed to determine their safety profile using the QikProp 4.4 tool of Maestro software [34]. Further, 9 compounds were selected from ADME property prediction. The QikProp parameters for the compounds are within the permitted range, as shown in Table 3. Thus, these 9 compounds were preceded for further analysis.

Table 3. ADME property prediction of 9 short-listed compounds.

Compounds name	QPlo gS	CIQPlo gS	QPPCa co	#meta b	ro3	CNS	QPlog BB	QPlog Kp	Jm	QPlog Khsa	QPlog HERG
Kaempferol	-2.390	-1.571	140.305	6	0	-2	-1.387	-1.387	0.029	-0.597	-3.346
Maritimetin	-2.117	-1.576	131.511	6	0	-2	-1.579	-4.495	0.074	-0.719	-3.542
N-(3-Benzooxazol-2-yl-4-hydroxy-phenyl)-2-ptolyloxyacetamide	-2.463	-1.269	73.938	4	0	0	-0.067	-0.067	0.000	0.013	-6.180
2,6-dihydroxybenzoic acid	-0.781	-0.568	306.522	2	0	-1	-0.951	-0.951	2.860	-0.843	-2.579
Methyl N-methylanthranilate	-0.127	0.028	1035.439	1	0	1	0.423	0.423	15.114	-0.541	-3.171
Gallic acid	-0.899	-0.473	86.213	3	0	-2	-1.472	-4.948	0.253	-0.868	-2.660
Vanillic acid	-1.065	-0.654	592.340	1	0	-1	-0.781	-0.781	5.814	-0.833	-3.022
Resorcinol	-0.677	-0.537	1128.290	2	0	0	-0.305	-0.305	13.232	-0.696	-2.476
2-Hydroxy-3-chloropenta-2,4- dienoate	-0.651	-0.774	554.543	1	0	-1	-0.704	-3.377	14.515	-0.894	-2.731

3.7. Binding free energy calculation.

MM-GBSA is a very popular method for predicting the binding affinity of compounds to proteins. The 9 compounds are evaluated for binding affinity with protein. The MM-GBSA

result illustrated that all 9 compounds show the highest negative values, which implies the strongest binding affinity between protein and ligand molecule. The relative binding free energies (G bind) of each ligand molecule were shown using the prime MMGBSA (Molecular mechanics-generalized Born surface area) technique [14], and the findings are shown in Table 4.

Table 4. Predicted MM-GBSA free binding energy score.

Compounds	Targeted proteins	MMGBSA-dG-binding energy (kcal/mol)	MMGBSA-dG-binding coulomb (kcal/mol)	MMGBSA-dG-bind(NS) (kcal/mol)	MMGBSA-dG-bind(NS) coulomb (kcal/mol)
Kaempferol	IL-6	-36.57	-11.70	-39.05	-14.23
	IL-1beta	-40.19	-14.94	-68.21	-16.31
	TNF-alpha	-54.28	-11.93	-73.15	-20.57
Maritimetin	IL-6	-36.96	-13.26	-46.27	-22.84
	IL-1beta	-64.07	-25.92	-70.37	-28.82
	TNF-alpha	-40.97	-13.05	-58.96	-18.86
N-(3-Benzooxazol-2-yl-4-hydroxy-phenyl)-2-p-tolyloxyacetamide	IL-6	-52.93	1.86	-68.13	-9.54
	IL-1beta	-69.13	78.03	-95.71	77.15
	TNF-alpha	-74.80	1.99	-95.72	4.26
2,6-dihydroxybenzoic acid	IL-6	-13.08	1.28	-12.16	2.35
	IL-1beta	-39.97	-27.43	-41.29	-29.45
Methyl N- methyl anthranilate	IL-6	-21.43	-63.02	-25.90	-64.66
	IL-1beta	-52.08	-6.88	-55.81	-7.86
Gallic acid	IL-6	-10.09	-9.51	-21.18	-19.84
	IL-1beta	-39.28	-26.42	-43.08	-26.58
Vanillic acid	IL-6	-28.86	-15.77	-28.94	-11.99
	IL-1beta	-45.00	-20.94	-50.97	-24.69
Resorcinol	IL-6	-11.37	-1.11	-11.45	-0.10
2-Hydroxy-3-chloropenta-2,4- dienoate	IL-1beta	-41.19	-28.56	-95.72	4.26

Table 5. Toxicology prediction of short-listed 7 compounds.

Compounds	Predicted LD50 MG/kg	Toxicity class	Hepato toxicity	Carcinogenicity	Immuno toxicity	Mutagenicity	Cytotoxicity
Kaempferol	3919	5	Inactive	Inactive	Inactive	Inactive	Inactive
Maritimetin	500	4	Inactive	Active	Active	Active	Inactive
N-(3-Benzooxazol-2-yl-4-hydroxy-phenyl)-2-ptolyloxyacetamide	1600	4	Mild active	Inactive	Inactive	Inactive	Inactive
2,6-dihydroxybenzoic acid	1250	4	Inactive	Inactive	Inactive	Inactive	Inactive
Methyl N- methyl anthranilate	2910	4	Mild active	Mild active	Inactive	Inactive	Inactive
Gallic acid	2000	5	Inactive	Mild active	Inactive	Inactive	Inactive
Vanillic acid	2000	4	Inactive	Inactive	Inactive	Inactive	Inactive
Resorcinol	200	3	Inactive	Inactive	Inactive	Inactive	Inactive
2-Hydroxy-3-chloropenta-2,4- dienoate	320	4	Inactive	Inactive	Inactive	Active	Inactive

3.8. Toxicity prediction.

The toxicity predicted of nine short-listed compounds was predicted using the Protox-II online tool. A toxicology investigation was carried out to forecast the safety features of compounds [35]. The main toxicity endpoints were considered, and the medications that did not adhere to the safety guidelines for toxicity endpoints were not taken into further consideration in our priority list. All 7 compounds are non-toxic because they are in 4, 5, and 6 toxicity classes and inactive in hepatotoxicity, carcinogenicity, immunotoxicity, mutagenicity, and cytotoxicity. The finalized 7 compounds are Kaempferol; N-(3-Benzooxazol-2-yl-4- hydroxy-phenyl)-2-p-tolyloxyacetamide; 2,6-Dihydroxybenzoic acid; Methyl N- methylanthranilate; Gallic acid; Vanillic acid; and Resorcinol are showing best compounds for further studies.

3.9. Hydrogen bond interaction.

According to the study, 7 compounds namely Kaempferol; N-(3-Benzooxazol-2-yl-4-hydroxy-phenyl)-2-p-tolyloxyacetamide; 2,6-Dihydroxybenzoic acid; Methyl N- methylanthranilate; Gallic acid; Vanillic acid; and Resorcinol are considered as targeted drugs because of good binding interaction with targeted proteins. Kaempferol [36] exhibited 4, 5, and 3 hydrogen bond interactions with IL-6, IL-1beta, and TNF-alpha. N-(3-Benzooxazol-2-yl-4-hydroxy-phenyl)-2-p-tolyloxyacetamide [37] is showing good binding interaction with 3 targets such as IL-6, IL-1beta, and TNF-alpha. The ligands interacted with the various residues surrounding the active pocket through hydrophobic, hydrogen-bonding, and other interactions. Compound 2,6-Dihydroxybenzoic acid [38] exhibited 2 and 3 hydrogen bond interactions with IL-6 and IL-1beta, respectively. Methyl N- methyl anthranilate [39] shows 2 and 1 hydrogen bond interaction with IL-6 and IL-1beta, respectively. Gallic acid [40] exhibited 5 hydrogen bond interactions with IL-6 and IL-1beta. Vanillic acid [41] revealed 3 hydrogen bond interactions with IL-6 and IL-1beta targets. Resorcinol [42] exhibited 2 hydrogen bond interactions with IL-6. Finally, Kaempferol and N-(3-Benzooxazol-2-yl-4- hydroxy-phenyl)-2-p-tolyloxyacetamide compounds are considered multi-targeted drugs.

Table 6. Hydrogen bond interaction with selected targets.

Sl. No	Name of compound	Targeted pro-inflammatory cytokines	Number of hydrogen bond	Residue concerned with hydrogen bond
1	Kaempferol	IL-6	4	ARG182, GLN175, SO4291
		IL-1beta	5	ARG B:2, PRO B:26, LEU B: 15, ILE B:13, GLU B: 11
		TNF-alpha	3	TYR C:227,SER C:136, TYR A:195
2	N-(3-Benzooxazol-2-yl-4-hydroxy-phenyl)-2-p-tolyloxyacetamide	IL-6	4	ASP34, GLN175
		IL-1beta	2	PRO B:26, GLU A:128
		TNF-alpha	1	LEU A:23
3	2,6-Dihydroxybenzoic acid	IL-6	2	SO4290, SO4291
		IL-1beta	3	ILE B:13 GLU B:11
4	Methyl N- methyl anthranilate	IL-6	2	SO4290, SO4291
		IL-1beta	1	PRO B:26
5	Gallic acid	IL-6	5	SER176, SO4290, SO4291
		IL-1beta	5	GLU B:11, ILE B:13, ILU B:15, ARG B:25, PRO B:26
6	Vanillic acid	IL-6	3	ASP25, ARG30, ARG182
		IL-1beta	3	ILE B:13, TYR B:127, PRO B:26
7	Resorcinol	IL-6	2	SO4290, SO4291

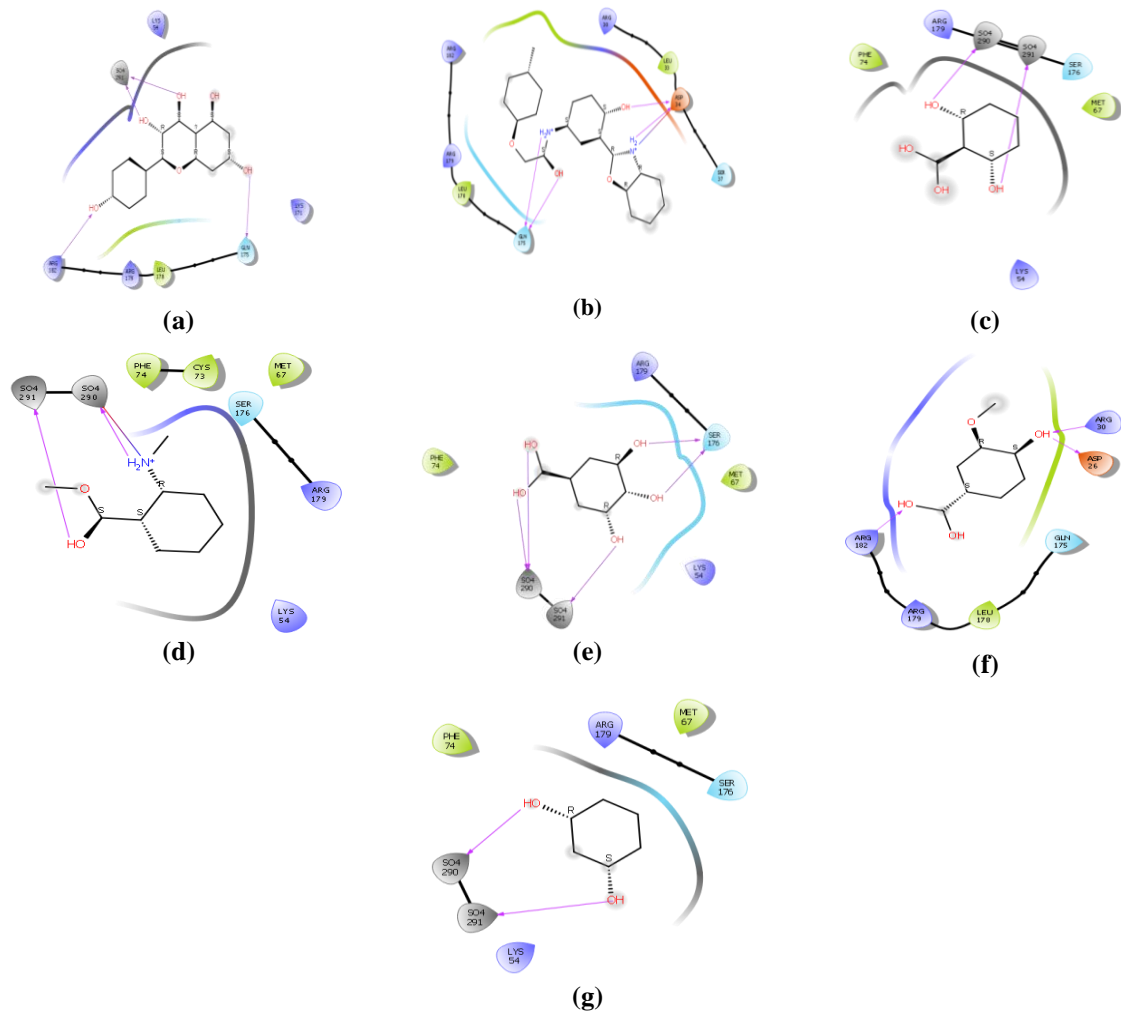


Figure 3. 2D structure of hydrogen bond interaction of bioactive compounds with pro-inflammatory receptor IL-6 (a) Kaempferol; (b) N-(3-Benzooxazol-2-yl-4-hydroxy-phenyl)-2-p-toloxacetamide; (c) 2,6-Dihydroxybenzoic acid; (d) Methyl N-methylantranilate; (e) Gallic acid; (f) Vanillic acid; (g) Resorcinol.

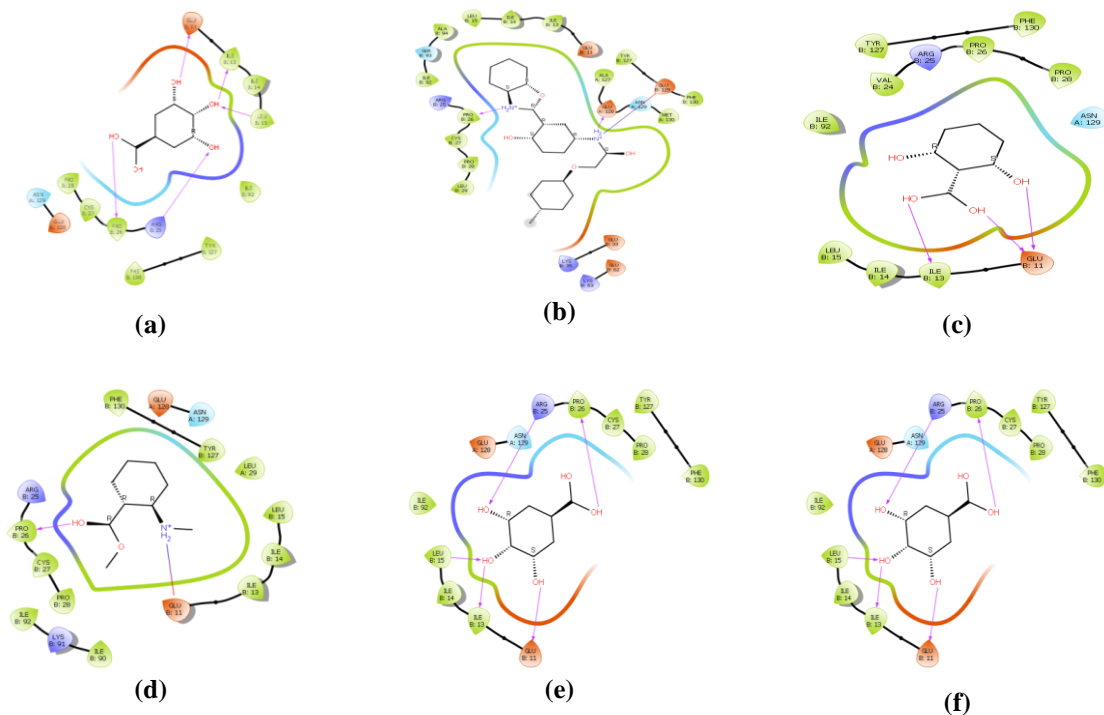


Figure 4. 2D structure of hydrogen bond interaction of bioactive compounds with pro-inflammatory receptor IL-1beta (a) Kaempferol; (b) N-(3-Benzooxazol-2-yl-4-hydroxy-phenyl)-2-p-toloxacetamide; (c) 2,6-Dihydroxybenzoic acid; (d) Methyl N-methylantranilate; (e) Gallic acid; (f) Vanillic acid.

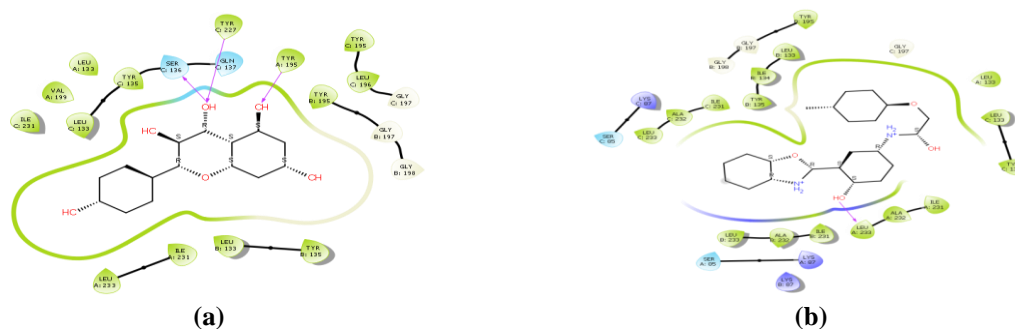


Figure 5. 2D structure of hydrogen bond interaction of bioactive compounds with pro-inflammatory receptor TNF-alpha (a) Kaempferol; (b) N-(3-Benzooxazol-2-yl-4- hydroxy-phenyl)-2-p-tolyloxyacetamide.

4. Conclusions

Present research work, virtual screening, *in silico* ADMET, and molecular docking studies were carried out to identify the possible bioactive phytoconstituents against pro-inflammatory cytokines using HR-LCMS analysis and *in silico* techniques. Target of the early responsive pro-inflammatory cytokines such as IL-1beta, IL-6, and TNF-alpha were selected for the study. The phytochemical signature was analyzed, and based on the results of HR-LCMS, 85 phytochemical constituents obeyed the Lipinski rule of five. These compounds were subjected to molecular docking with pro-inflammatory targets. The 11 compounds show good binding energy with 1,2,3,4, and 5 hydrogen bond interaction with three targets, and the 9 compounds have values for each parameter that are within the range based on the ADME prediction, and 7 compounds are considered non-toxic based on toxicity prediction. This work suggests that the 7 compounds, namely Kaempferol; N-(3-Benzooxazol-2-yl-4- hydroxy-phenyl)-2-ptolyloxyacetamide; 2,6-Dihydroxybenzoic acid; Methyl N- methylanthranilate; Gallic acid; Vanillic acid; and Resorcinol are found as potential bioactive compounds inhibiting pro-inflammatory targets IL-6, IL-1beta and TNF-alpha. All seven compounds are inhibiting IL-6, six are inhibiting IL-1beta, and two are inhibiting TNF-alpha. The Kaempferol and N-(3-Benzooxazol-2-yl-4- hydroxy-phenyl)-2-ptolyloxyacetamide compounds are inhibiting all three early responsive cytokines; hence, these two molecules are possibly considered as multi-targeted drugs for inflammatory diseases. Further, *in vitro* and *in vivo* validation of these compounds may explore treatment regimes for managing inflammatory diseases.

Funding

This research received no external funding.

Acknowledgments

Authors wish to acknowledge DBT-BIF, Govt. of India, and K-FIST L1, VGST, Govt. of Karnataka, for providing a facility for molecular docking and acknowledging Karnataka State Akkamahadevi Women's University for providing an infrastructure facility.

Conflicts of Interest

The authors declare no conflict of interest.

References

1. Ekor, M. The growing use of herbal medicines: issues relating to adverse reactions and challenges in monitoring safety. *Front. Pharmacol.* **2014**, *4*, 177, <https://doi.org/10.3389/fphar.2013.00177>.
2. Anand, U., Tudu, C. K., Nandy, S., Sunita, K., Tripathi, V., Loake, G. J., ... & Proćków, J. Ethnodermatological use of medicinal plants in India: From ayurvedic formulations to clinical perspectives—A review. *Journal of ethnopharmacology*, **2022**, *284*, 114744.
3. Nawaz, M.P.; Ramamurthy, V.; Rajamohamed, S. STUDY OF THE PHYTOCHEMICAL ANALYSIS AND ANTIMICROBIAL ACTIVITY OF CASSIA AURICULATA. *World J. Pharm. Res.* 2017, *6*, 523-531.
4. Gupta, A.K.; Tandon, N.; Sharma, M.; Indian Council of Medical, R. Quality Standards of Indian Medicinal Plants; Indian Council of Medical Research: **2009**.
5. Surana, S.J.; Gokhale, S.B.; Jadhav, R.B.; Sawant, R.L.; Wadekar, J.B. Antihyperglycemic Activity of Various Fractions of *Cassia auriculata* Linn. in Alloxan Diabetic Rats. *Indian J. Pharm. Sci.* **2008**, *70*, 227-229, <https://doi.org/10.4103/0250-474x.41461>.
6. Rajagopal, A.; Rajakannu, S. *Cassia auriculata* and its role in infection / inflammation: A close look on future drug discovery. *Chemosphere* **2022**, *287*, 132345, <https://doi.org/10.1016/j.chemosphere.2021.132345>.
7. Chanderraj, P. In vitro antioxidant activities and molecular docking of *Cassia auriculata* medicinal plant. *Res. J. Biotechnol.* **2023**, *18*, 107-111.
8. Chen, L.; Deng, H.; Cui, H.; Fang, J.; Zuo, Z.; Deng, J.; Li, Y.; Wang, X.; Zhao, L. Inflammatory responses and inflammation-associated diseases in organs. *Oncotarget* **2018**, *9*, 7204-7218, <https://doi.org/10.18632/oncotarget.23208>.
9. Hurley, J.V. Acute Inflammation: The Effect of Concurrent Leucocytic Emigration and Increased Permeability on Particle Retention by the Vascular Wall. *Br. J. Exp. Pathol.* **1964**, *45*, 627-633.
10. Ricciotti, E.; FitzGerald, G.A. Prostaglandins and inflammation. *Arterioscler. Thromb. Vasc. Biol.* **2011**, *31*, 986-1000, <https://doi.org/10.1161/atvbaha.110.207449>.
11. Chavan, M.J.; Wakte, P.S.; Shinde, D.B. Analgesic and anti-inflammatory activities of 18-acetoxy-ent-kaur-16-ene from *Annona squamosa* L. bark. *Inflammopharmacology* **2011**, *19*, 111-115, <https://doi.org/10.1007/s10787-010-0061-5>.
12. Binatti, E.; Gerussi, A.; Barisani, D.; Invernizzi, P. The Role of Macrophages in Liver Fibrosis: New Therapeutic Opportunities. *Int. J. Mol. Sci.* **2022**, *23*, 6649, <https://doi.org/10.3390/ijms23126649>.
13. Luna-Rodríguez, C.E.; González, G.M.; Flores-Maldonado, O.E.; Treviño-Rangel, R.; Rosas-Taraco, A.G.; Becerril-García, M.A. Early production of proinflammatory cytokines in response to *Scedosporium apiospermum* during murine pulmonary infection. *Microb. Pathog.* **2022**, *170*, 105718, <https://doi.org/10.1016/j.micpath.2022.105718>.
14. Petrenko, D.E.; Timofeev, V.I.; Karlinsky, D.M.; Plashchinskaia, D.D.; Mikhailova, A.G.; Rakitina, T.V. Study of the Binding Free Energy of Peptide Substrates in the Active Site of Oligopeptidase B from *Serratia proteamaculans* by the MM-GBSA Method. *Crystallogr. Rep.* **2022**, *67*, 383-390, <https://doi.org/10.1134/S1063774522030154>.
15. Raja, D.K.; Jeganathan, N.S.; Manavalan, R. In vitro antimicrobial activity and phytochemical analysis of *Cassia auriculata* Linn. *Int. Curr. Pharm. J.* **2013**, *2*, 105-108, <https://doi.org/10.3329/icpj.v2i6.14869>.
16. Ramakrishnan, P.; Kalakandan, S.; Pakkirisamy, M. Studies on Positive and Negative ionization mode of ESI-LC-MS/ MS for screening of Phytochemicals on *Cassia auriculata* (Aavaram Poo). *Pharmacogn. J.* **2018**, *10*, 457-462.
17. Kim, S.; Thiessen, P.A.; Bolton, E.E.; Chen, J.; Fu, G.; Gindulyte, A.; Han, L.; He, J.; He, S.; Shoemaker, B.A.; Wang, J.; Yu, B.; Zhang, J.; Bryant, S.H. PubChem Substance and Compound databases. *Nucleic Acids Res.* **2016**, *44*, D1202-D1213, <https://doi.org/10.1093/nar/gkv951>.
18. Madhavi Sastry, G.; Adzhigirey, M.; Day, T.; Annabhimoju, R.; Sherman, W. Protein and ligand preparation: parameters, protocols, and influence on virtual screening enrichments. *J. Comput.-Aided Mol. Des.* **2013**, *27*, 221-234, <https://doi.org/10.1007/s10822-013-9644-8>.
19. Mohd Amin, S.N.; Md Idris, M.H.; Selvaraj, M.; Mohd Amin, S.N.; Jamari, H.; Kek, T.L.; Salleh, M.Z. Virtual screening, ADME study, and molecular dynamic simulation of chalcone and flavone derivatives as 5-Lipoxygenase (5-LO) inhibitor. *Mol. Simul.* **2020**, *46*, 487-496, <https://doi.org/10.1080/08927022.2020.1732961>.

20. Litov, L.; Petkov, P.; Rangelov, M.; Ilieva, N.; Lilkova, E.; Todorova, N.; Krachmarova, E.; Malinova, K.; Gospodinov, A.; Hristova, R.; Ivanov, I.; Nacheva, G. Molecular Mechanism of the Anti-Inflammatory Action of Heparin. *Int. J. Mol. Sci.* **2021**, *22*, 10730, <https://doi.org/10.3390/ijms221910730>.
21. Wang, S.; Ji, L.; Zhang, D.; Guo, H.; Wang, Y.; Li, W. Synthesis and Anti-Inflammatory Activity of 1-Methylhydantoin Cinnamoyl Imides. *Molecules* **2022**, *27*, 8481, <https://doi.org/10.3390/molecules27238481>.
22. Bae, C. H., Kim, H. Y., Seo, J. E., Lee, H., & Kim, S.. In Silico Analysis of Pyeongwi-San Involved in Inflammatory Bowel Disease Treatment Using Network Pharmacology, Molecular Docking, and Molecular Dynamics. *Biomolecules*, **2023**, *13*(9), 1322.
23. Bittrich, S.; Rose, Y.; Segura, J.; Lowe, R.; Westbrook, J.D.; Duarte, J.M.; Burley, S.K. RCSB Protein Data Bank: improved annotation, search and visualization of membrane protein structures archived in the PDB. *Bioinformatics* **2022**, *38*, 1452-1454, <https://doi.org/10.1093/bioinformatics/btab813>.
24. Ge, Y.; Ganamet, K. Using sitemap to aid in the identification of cryptic binding pockets. *Biophys. J.* **2023**, *122*, 142a.
25. Yadav, R.; Imran, M.; Dhamija, P.; Suchal, K.; Handu, S. Virtual screening and dynamics of potential inhibitors targeting RNA binding domain of nucleocapsid phosphoprotein from SARS-CoV-2. *J. Biomol. Struct. Dyn.* **2021**, *39*, 4433-4448, <https://doi.org/10.1080/07391102.2020.1778536>.
26. Pandi, S.; Kulanthaivel, L.; Subbaraj, G.K.; Rajaram, S.; Subramanian, S. Screening of Potential Breast Cancer Inhibitors through Molecular Docking and Molecular Dynamics Simulation. *Biomed Res. Int.* **2022**, *2022*, 3338549, <https://doi.org/10.1155/2022/3338549>.
27. Banerjee, P.; Eckert, A.O.; Schrey, A.K.; Preissner, R. ProTox-II: a webserver for the prediction of toxicity of chemicals. *Nucleic Acids Res.* **2018**, *46*, W257-W263, <https://doi.org/10.1093/nar/gky318>.
28. Murad, H.A.S.; Alqurashi, T.M.A.; Hussien, M.A. Interactions of selected cardiovascular active natural compounds with CXCR4 and CXCR7 receptors: a molecular docking, molecular dynamics, and pharmacokinetic/toxicity prediction study. *BMC Complement. Med. Ther.* **2022**, *22*, 35, <https://doi.org/10.1186/s12906-021-03488-8>.
29. Kalirajan, R.; Pandiselvi, A.; Gowramma, B.; Balachandran, P. In-silico Design, ADMET Screening, MM-GBSA Binding Free Energy of Some Novel Isoxazole Substituted 9-Anilinoacridines as HER2 Inhibitors Targeting Breast Cancer. *Curr. Drug Res. Rev.* **2019**, *11*, 118-128, <https://doi.org/10.2174/2589977511666190912154817>.
30. Ongaro, A.; Oselladore, E.; Memo, M.; Ribaudo, G.; Gianoncelli, A. Insight into the LFA-1/SARS-CoV-2 Orf7a Complex by Protein-Protein Docking, Molecular Dynamics, and MM-GBSA Calculations. *J. Chem. Inf. Model.* **2021**, *61*, 2780-2787, <https://doi.org/10.1021/acs.jcim.1c00198>.
31. Rafiq, S.; Wagay, N.A.; Elansary, H.O.; Malik, M.A.; Bhat, I.A.; Kaloo, Z.A.; Hadi, A.; Alataway, A.; Dewidar, A.Z.; El-Sabrou, A.M.; Yessoufou, K.; Mahmoud, E.A. Phytochemical Screening, Antioxidant and Antifungal Activities of *Aconitum chasmanthum* Stapf ex Holmes Wild Rhizome Extracts. *Antioxidants* **2022**, *11*, 1052, <https://doi.org/10.3390/antiox11061052>.
32. Chen, C.-K.; Leung, S.S.F.; Guillbert, C.; Jacobson, M.P.; McKerrow, J.H.; Podust, L.M. Structural Characterization of CYP51 from *Trypanosoma cruzi* and *Trypanosoma brucei* Bound to the Antifungal Drugs Posaconazole and Fluconazole. *PLOS Negl. Trop. Dis.* **2010**, *4*, e651, <https://doi.org/10.1371/journal.pntd.0000651>.
33. Shelley, J.C.; Cholleti, A.; Frye, L.L.; Greenwood, J.R.; Timlin, M.R.; Uchimaya, M. Epik: a software program for pK_a prediction and protonation state generation for drug-like molecules. *J. Comput.-Aided Mol. Des.* **2007**, *21*, 681-691, <https://doi.org/10.1007/s10822-007-9133-z>.
34. Bharadwaj, K.K.; Ahmad, I.; Pati, S.; Ghosh, A.; Rabha, B.; Sarkar, T.; Bhattacharjya, D.; Patel, H.; Baishya, D. Screening of Phytochemicals for Identification of Prospective Histone Deacetylase 1 (HDAC1) Inhibitor: An In Silico Molecular Docking, Molecular Dynamics Simulation, and MM-GBSA Approach. *Appl. Biochem. Biotechnol.* **2024**, *196*, 3747-3764, <https://doi.org/10.1007/s12010-023-04731-3>.
35. Divya Rajaselvi, N.; Jida, M.D.; Nair, D.B.; Sujith, S.; Beegum, N.; Nisha, A.R. Toxicity prediction and analysis of flavonoid apigenin as a histone deacetylase inhibitor: an in-silico approach. *In Silico Pharmacology* **2023**, *11*, 34, <https://doi.org/10.21203/rs.3.rs-3149173/v1>.
36. Bangar, S.P.; Chaudhary, V.; Sharma, N.; Bansal, V.; Ozogul, F.; Lorenzo, J.M. Kaempferol: A flavonoid with wider biological activities and its applications. *Crit. Rev. Food Sci. Nutr.* **2023**, *63*, 9580-9604, <https://doi.org/10.1080/10408398.2022.2067121>.

37. Kondratov, R.V.; Komarov, P.G.; Becker, Y.; Ewenson, A.; Gudkov, A.V. Small molecules that dramatically alter multidrug resistance phenotype by modulating the substrate specificity of P-glycoprotein. *Proc. Natl. Acad. Sci.* **2001**, *98*, 14078-14083, <https://doi.org/10.1073/pnas.241314798>.
38. Dewel, D.; Metzger, H. 2,6-Dihydroxybenzoic acid anilides as fasciolicides. *J. Med. Chem.* **1973**, *16*, 433-436, <https://doi.org/10.1021/jm00263a001>.
39. Silva, C.A.O.; Freitas, V.L.S.; da Silva, M.D.M.C.R. Determination and Analysis of Thermodynamic Properties of Methyl Methylantranilate Isomers. *Molecules* **2023**, *28*, 6686, <https://doi.org/10.3390/molecules28186686>.
40. Bai, J.; Zhang, Y.; Tang, C.; Hou, Y.; Ai, X.; Chen, X.; Zhang, Y.; Wang, X.; Meng, X. Gallic acid: Pharmacological activities and molecular mechanisms involved in inflammation-related diseases. *Biomed. Pharmacother.* **2021**, *133*, 110985, <https://doi.org/10.1016/j.biopha.2020.110985>.
41. Malik, A.; Khatkar, A.; Kakkar, S. A Review on Pharmacological Activities of Vanillic Acid and its Derivatives. *Indo Global J. Pharm. Sci.* **2023**, *13*, 1-12, <https://doi.org/10.35652/IGJPS.2023.13001>.
42. Rahen, M.; De Tran, Q.; Negar, S.S.; Khadija, A.P.; Pranoy, S.; Sukumar, B.; Shahenul, I.; Shamima, A. In vitro anti-inflammatory resorcinol derivatives and their *in silico* analysis. *Can Tho Univ. J. Sci.* **2020**, *12*, 80-84, <https://doi.org/10.22144/ctu.jen.2020.027>.